Thermophysical properties of undercooled liquid Au–Cu alloys from molecular dynamics simulations

Thermophysical properties of undercooled liquid Au–Cu alloys from molecular dynamics simulations

X J Han, M Chen[1] and Z Y Guo

Department of Engineering Mechanics, Tsinghua University, Beijing 100084, People's Republic of China

E-mail: mchen@tsinghua.edu.cn

Abstract
The density and the specific heat of liquid Au–Cu alloy above and below the melting temperature are investigated in a wide composition range via constant temperature and constant pressure molecular dynamics simulations. The atomic interaction of the alloy is described with the embedded-atom method (EAM). The equilibrium melting temperature is evaluated from the change in the growth direction of a crystal–liquid sandwich structure under annealing. The simulated density of the Au–Cu alloy increases linearly with decrease of the temperature, whereas the specific heat remains constant over the entire temperature range of 900–1900 K. The excess volume is calculated according to the predicted density of Au–Cu alloy. The negative value of the excess volume and the exponential concentration dependence of the specific heat indicate that the Neumann–Kopp rule does not apply to the Au–Cu binary alloy system.

1. Introduction

Thermophysical properties of undercooled liquid alloys are important both for fundamental understanding and for industrial practices of material preparation [1, 2]. Unfortunately, it is very difficult to measure thermophysical properties of undercooled liquid alloys with high melting points. This is mainly because at high temperatures any physical contact between the alloy melt and the container will induce immediate nucleation, and thus the metastable state of deep undercooling is hard to access. Therefore, up to now, few experimental studies of thermophysical properties of undercooled liquid alloys, even for the most important properties, i.e., density and specific heat, have been carried out. As an alternative to obtaining thermophysical property experimentally, attempts have also been made to develop predictive methods during the past few decades. Among the methods, molecular dynamics (MD) simulation is considered to be one of the most promising [3, 4]. The existing applications of MD to thermophysical properties include those to transition metals [5, 6], main group

---

[1] Author to whom any correspondence should be addressed.

metals [7] and some rare earth metals [8]. Meanwhile, important progress has also been made in the MD study of some binary alloys such as Ni–Zr [9, 10].

Thermodynamic melting temperature T_m plays an important role in the computer simulation of thermophysical properties of undercooled liquid alloys, since we cannot determine whether the liquid alloy is in the normal state or in a metastable undercooled state without the knowledge of T_m. T_m can be estimated by a MD simulation of a metastable crystal–liquid sandwich structure and by studying the growth direction of the layers as a function of temperature. This approach is well established in early MD simulations [11, 12] and was recently applied successfully to simulate the melting transition of $Ni_{0.5}Zr_{0.5}$ intermetallic compound [10].

Au–Cu is a well-known 'model' binary alloy system, which is famous for the existence of a temperature-induced order–disorder transition and the capability of forming thermodynamically stable long period superlattice structure. In addition, three intermetallic compounds, namely Au_3Cu, $AuCu$ and $AuCu_3$, are of potential use in industry due to their high melting temperature, high strength and high corrosion resistance properties. Though plenty of research has focused on this alloy system both experimentally and theoretically [13–16], little attention has been paid to the thermophysical properties of undercooled liquid Au–Cu alloys, systematically.

The purpose of this paper is to predict the density and specific heat of undercooled liquid Au–Cu alloys in a wide composition range by a molecular dynamics method. Au, Au_3Cu, $AuCu$, $AuCu_3$ and Cu are chosen for investigation. The equilibrium melting temperature is estimated from the growth direction in layered crystal–liquid computer modelled structures.

2. Inter-atomic potential

The inter-atomic potential of a metal or alloy forms the basis of a molecular dynamics simulation. The embedded-atom method (EAM) proposed by Daw and Baskes [17, 18], based on the quasi-atom concept and the density function theory, has achieved great success in describing the interaction of atoms of metals and alloys. It has been applied in the prediction of thermal expansion, surface, liquid structure, the liquid–glass transition and crystal growth.

In the EAM, the energy of a system is subdivided into the embedding energy, i.e. the energy required to embed an atom into the local electron density due to the background atoms, and the core–core repulsion:

$$E_{tot} = \sum_i F_i(\rho_i) + \frac{1}{2} \sum_{i \neq j} \phi_{i,j}(r_{i,j}) \tag{1}$$

$$\rho_i = \sum_{i \neq j} f_j(r_{i,j}) \tag{2}$$

where E_{tot} is the total internal energy, F_i the energy for embedding atom i in an electron density ρ_i, $\phi_{i,j}$ the repulsive two-body potential between atoms i and j, $r_{i,j}$ the separation distance between atoms i and j and $f_j(r_{i,j})$ the contribution of atom j to the electron density at atom i at a distance $r_{i,j}$ from atom j.

Recently, Barrera put forward an EAM model for Au–Cu alloys [19], which was fitted to room-temperature experimental data and took vibrational contributions into account. This model has been applied successfully to describe the characteristics of the order–disorder transition and the structures and cohesive energies of Au–Cu alloys. According to this model, the electronic densities, the repulsive potential and the embedding energy are represented as

$$f_j(r) = A_j \exp(-r/\sigma_j^e) \tag{3}$$

Table 1. Parameters of the potential model of Au–Cu alloys.

i/j	B_{ij}	σ_{ij}^{r} (Å)	A_i	σ_{ij}^{e} (Å)	C_i (eV)
Cu	7 076.56	0.241 535	188.542	0.536 562	1
Au	14 759.9	0.272 639	4162.93	0.366 085	1.421 97
Cu/Au	10 153.2	0.258 268			

$$\phi_{ij}(r) = B_{ij}\exp(-r_{ij}/\sigma_{ij}^{\mathrm{r}}) \tag{4}$$
$$F_j(\rho_j) = -C_j\sqrt{\rho_j}. \tag{5}$$

The model parameters are listed in table 1.

3. Simulation details

3.1. Density and specific heat

MD simulations were performed in face-centred cubic boxes subject to periodic boundary conditions for systems with 500–2048 particles. The numbers of the gold atoms and the copper atoms were assigned according to their atomic percentage in the Au–Cu alloys. In the simulation, the isothermal and isobaric ensemble was used and the pressure was set to zero. The time step was set as 4.15 fs. In order to get an equilibrium liquid state in the simulation, the system started at 1900 K, which is well above the equilibrium melting temperatures of Cu, AuCu$_3$, AuCu, Au$_3$Cu and Au. This temperature was kept constant for 50 000 time steps. Then the quenching process with a cooling rate of 4.82×10^{11} K s^{-1} was carried out to calculate the enthalpy H and density ρ at 100 K intervals of temperature. At each temperature, 30 000 steps were carried out to achieve equilibrium. Then 20 000 additional steps were taken to calculate the enthalpy and density. The simulations were stopped at 900 K. At this temperature, the four Au–Cu alloys are still in an undercooled liquid state due to the high cooling rate and the 'pure' circumstances in the simulation.

During the simulation, the density of the alloy was adjusted according to the feedback of the pressure's deviation from zero. The pressure was calculated with the expression [20]

$$P = \rho^* k_{\mathrm{B}} T + \frac{1}{3V}\left\langle\sum_{i<j} r_{ij}\cdot f_{ij}\right\rangle \tag{6}$$

where ρ^* is the number density, k_{B} the Boltzmann constant, T the temperature, $\langle\,\rangle$ the ensemble average, r_{ij} and f_{ij} the separation and force between atom i and atom j, respectively.

Specific heat can be determined from the differential of the enthalpy:

$$C_p = \mathrm{d}H(T)/\mathrm{d}T. \tag{7}$$

3.2. Equilibrium melting temperature T_m

During simulations of T_{m}, an orthorhombic box subject to periodical boundary conditions is filled with 1000 atoms. The ratio of box size with respect to x, y and z directions is 1:1:2. The initial configuration of particles is fixed in a crystal–liquid–crystal sandwich structure along the z-axis. The system along the z-axis is divided into 12 layers. The first and the last three layers hold 500 particles in the solid state and the intermediate six layers hold the rest of the 500 particles in the liquid state. The solid particles are in equilibrium after 30 000 time steps at 300 K and the liquid particles are in equilibrium after 50 000 time steps at 2300 K. Then the whole system was allowed to develop for 80 000 time steps at object temperatures. The
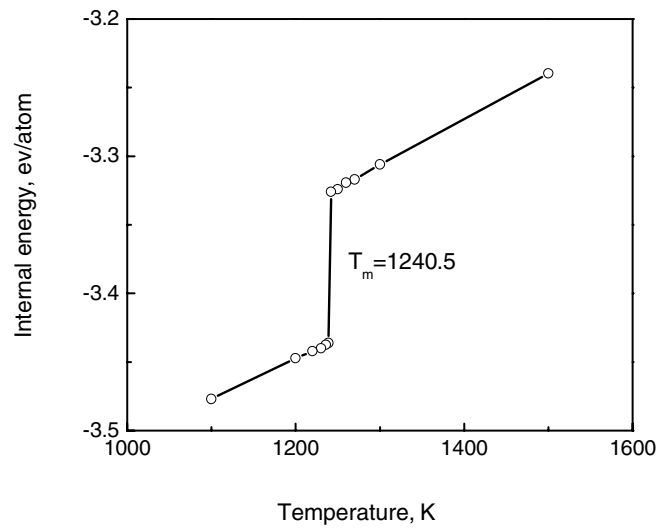
Figure 1. The calculated sandwich structure internal energy of AuCu$_3$ alloy at the end state versus temperature.

Table 2. Calculated and experimental T_m for Au–Cu alloys.

Au–Cu alloys	T_m^{Calc} (K)	T_m^{Exp} (K)	Deviation (%)
Cu	1320.5 ± 1.5	1356	−2.62
AuCu$_3$	1240.5 ± 1.5	1250	−0.76
AuCu	1173.5 ± 0.5	1185	−0.97
Au$_3$Cu	1151.5 ± 1.5	1220	−5.61
Au	1182.5 ± 1.5	1336	−11.49

equilibrium melting temperature is estimated from the change of the growth direction in the sandwich crystal–liquid computer modelled structures. Above T_m, the liquid phase will grow on account of the solid phase and below T_m vice versa.

4. Results and discussion

4.1. Equilibrium melting temperature T_m for Au–Cu alloys

Figure 1 presents the simulated internal energy E of AuCu$_3$ alloy in its homogeneous end state when starting with a crystal–liquid sandwich structure. Obviously, there exists a critical temperature $T_m = 1240.5 ± 1.5$ K in the E–T curve. The final configurations of the system indicate that below T_m the system crystallizes, while above T_m the system turns into homogeneous liquid. Therefore, T_m is the equilibrium melting temperature of AuCu$_3$ alloy at zero pressure. With the same method, the equilibrium melting temperatures of Cu, AuCu, Au$_3$Cu and Au were estimated. The simulated T_m and the experimental data taken from Au–Cu phase diagrams [21] are listed in table 2. Comparison shows a good agreement between the calculated and experimental T_m.

According to the predicted equilibrium melting temperatures, the maximum undercoolings obtained during simulations are 421, 341, 274, 253 and 283 K for Cu, AuCu$_3$, AuCu, Au$_3$Cu and Au, respectively.

Table 3. Predicted results for AuCu$_3$ alloy with systems of 500, 1372 and 2048 atoms.

	Density (kg m^{-3})			Enthalpy (10^6 J kg^{-1})		
T (K)	500	1372	2048	500	1372	2048
1900	10 146.01	10 145.45	10 146.47	−3.066 06	−3.065 92	−3.066 09
1800	10 265.49	10 269.31	10 270.90	−3.099 00	−3.100 19	−3.100 15
1700	10 391.21	10 393.31	10 394.38	−3.134 00	−3.134 45	−3.134 27
1600	10 510.01	10 516.07	10 515.99	−3.167 84	−3.168 82	−3.168 96
1500	10 640.17	10 640.94	10 639.38	−3.203 64	−3.203 74	−3.203 79
1400	10 759.90	10 765.06	10 765.66	−3.238 29	−3.238 99	−3.239 22
1300	10 888.10	10 892.23	10 890.37	−3.274 15	−3.275 05	−3.274 40
1200	11 019.09	11 020.73	11 019.66	−3.311 29	−3.311 36	−3.310 93
1100	11 143.80	11 146.18	11 149.96	−3.346 95	−3.347 41	−3.347 95
1000	11 274.89	11 280.92	11 277.64	−3.383 90	−3.385 38	−3.384 41
900	11 408.60	11 411.56	11 409.37	−3.421 45	−3.422 74	−3.422 56

Table 4. Predicted ρ_m and dρ/dT for Au–Cu alloys.

Au–Cu alloys	T_m (K)	ρ_m (kg m^{-3})	dρ/dT (kg m^{-3} K^{-1})
Cu	1320.5	7 867.5	−0.890 57
AuCu$_3$	1240.5	10 994.6	−1.239 33
AuCu	1173.5	13 489.7	−1.575 29
Au$_3$Cu	1151.5	15 456.8	−1.977 32
Au	1182.5	16 853.2	−2.412 28

4.2. Thermophysical properties of liquid Au–Cu alloys

Taking AuCu$_3$ alloy as an example, we first studied the influence of the computation scale on the simulated results. The predicted density and enthalpy of AuCu$_3$ alloy at different temperatures with systems of 500, 1372 and 2048 atoms are listed in table 3. Clearly, the results for these three systems are quite close. The differences of density and enthalpy are less than 0.06% and 0.04%, respectively. This indicates that the size effect of the simulation domain on the simulated thermophysical properties here is negligible and simulations with a system of 500 atoms are sometimes acceptable.

Figure 2 presents the predicted density of Au–Cu alloys versus temperature with a system of 500 atoms. Data analysis indicates that the density of Au–Cu alloys can be represented by a linear function of temperature T:

$$\rho = \rho_m + \frac{d\rho}{dT}(T - T_m) \tag{8}$$

where ρ_m is the density at equilibrium melting temperature T_m and dρ/dT is the temperature dependence of the density.

ρ_m, T_m and dρ/dT for Au–Cu alloys are listed in table 4. Obviously, both the magnitude of density and its temperature dependence increase with increase of the gold content. In order to evaluate the deviation between the prediction and the experimental data, the density of pure liquid copper and gold above their melting points from *Smithells Metals Reference Book* [22] are also superimposed upon figure 2. Comparisons show that the predicted results underestimate the experimental values slightly. At equilibrium melting temperatures, the differences are about 2% and 3% for pure liquid copper and gold respectively. The deviations of the calculated densities of AuCu$_3$, AuCu and Au$_3$Cu alloys are not evaluated due to the lack of experimental data on the liquid state.
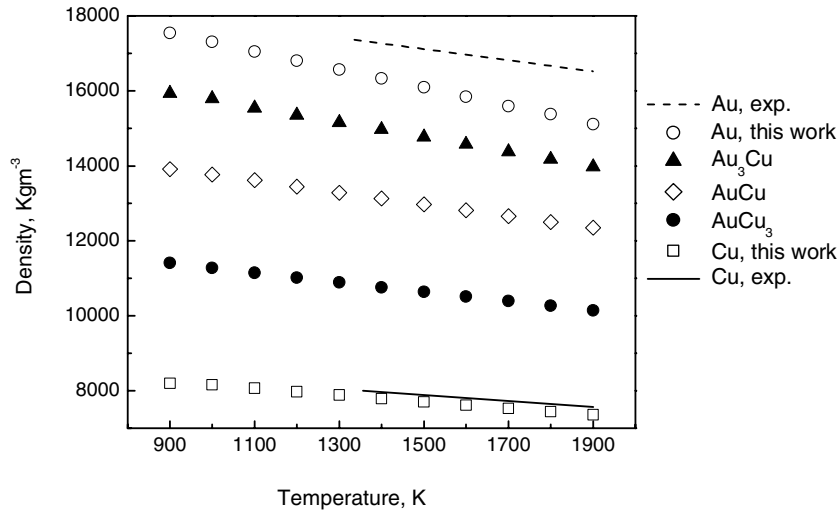
Figure 2. Density of Au–Cu alloys versus temperature.

Generally, when experimental data are not available, the density of liquid alloys is approximated from a linear interpolation of experimental data for pure elements according to the Neumann–Kopp rule. In order to check the deviation of this approximation for Au–Cu alloys, the excess volumes ΔV^{Ex} were calculated using the relation

$$\Delta V^{\mathrm{Ex}} = [x_1 M_1 + x_2 M_2]/\rho_{\mathrm{A}} - [x_1 M_1/\rho_1 + x_2 M_2/\rho_2] \tag{9}$$

where subscript 1 refers to gold and 2 to copper, ρ_{A} is the alloy density, x_i, M_i and ρ_i are the atomic fraction, atomic weight and density of components 1 and 2, respectively. The calculated ΔV^{Ex} for Au–Cu alloys are depicted in figure 3. For clarity, only the data at four temperatures, namely, 1000, 1300, 1600 and 1900 K, are illustrated. As shown in the figure, the Au–Cu binary alloy system exhibits a negative excess volume. This indicates that the liquid Au–Cu alloy deviates from the ideal solution and a linear approximation of the alloy density according to the Neumann–Kopp rule will cause negative deviation.

Like the density, the enthalpy of Au–Cu alloys is a linear function of temperature, as illustrated in figure 4:

$$H_{\mathrm{Cu}} = -5.426\,56 \times 10^6 + (530.03 \pm 2.97)T \ \mathrm{J\ kg}^{-1} \tag{10}$$

$$H_{\mathrm{AuCu_3}} = -3.738\,87 \times 10^6 + (351.38 \pm 1.65)T \ \mathrm{J\ kg}^{-1} \tag{11}$$

$$H_{\mathrm{AuCu}} = -2.860\,68 \times 10^6 + (262.79 \pm 1.66)T \ \mathrm{J\ kg}^{-1} \tag{12}$$

$$H_{\mathrm{Au_3Cu}} = -2.313\,58 \times 10^6 + (209.95 \pm 0.66)T \ \mathrm{J\ kg}^{-1} \tag{13}$$

$$H_{\mathrm{Au}} = -1.933\,80 \times 10^6 + (174.12 \pm 1.95)T \ \mathrm{J\ kg}^{-1}. \tag{14}$$

Accordingly, the specific heats of Au–Cu alloys within the simulation temperature range are 530.03 ± 2.97, 351.38 ± 1.65, 262.79 ± 1.66, 209.95 ± 0.66 and 174.12 ± 1.95 J kg^{-1} K^{-1}, respectively. The dependences of the specific heats of these five Au–Cu alloys on the gold content are given in figure 5. The specific heat for Au–Cu alloys C_{PL} increases exponentially as the atomic percentage of copper X_{Cu} increases:

$$C_{\mathrm{PL}} = 141.16 + 36.24 \exp(X_{\mathrm{Cu}}/42.19). \tag{15}$$

In order to evaluate the specific heat predicted from MD simulation, the experimental results of Bykov [23] for normal liquid Au–Cu alloys above the liquidus temperature are also shown
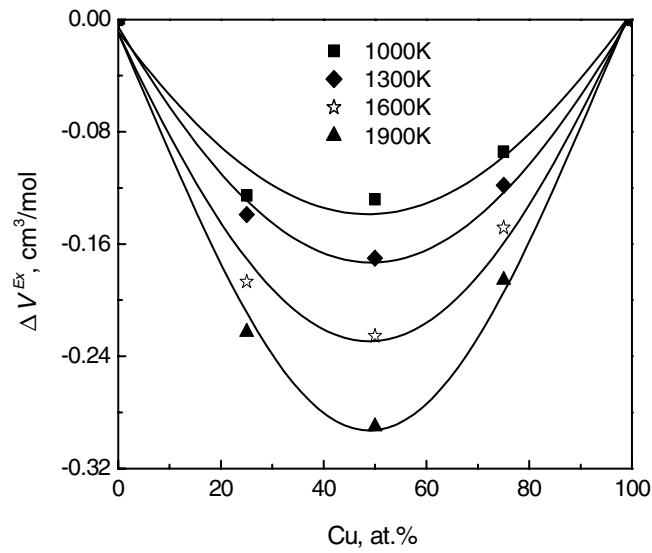
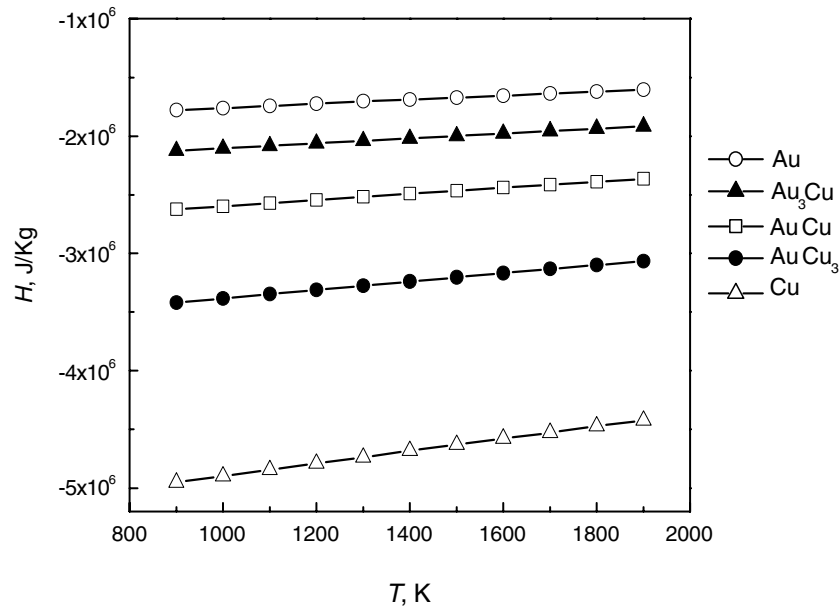**Figure 3.** Excess volume of Au–Cu alloys versus copper concentration.

Figure 4. Enthalpy of Au–Cu alloys versus temperature.

in figure 5. Comparisons indicate that the predicted specific heats of AuCu and AuCu$_3$ alloys are in excellent agreement with the experimental results of Bykov in the normal liquid regime. The predicted results for Au$_3$Cu and Cu slightly overestimate the experimental values, with discrepancies of about 11% and 7% respectively. Despite an almost 15% overestimation of the experimental data of Bykov above the melting point, the predicted specific heat of pure liquid gold in this work is quite close to Wilde's result of 165–168 J kg^{-1} K^{-1}, represented by

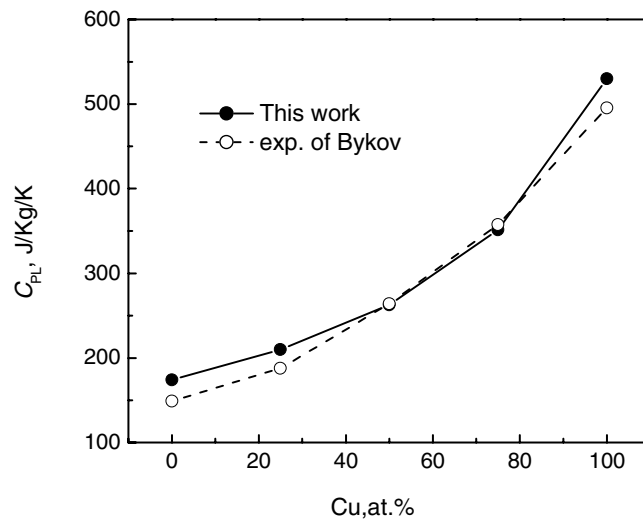**Figure 5.** Dependences of specific heats of Au–Cu alloys on the copper concentration.

$C_{PL} = 177 - 0.007\,98\,T$ J kg^{-1} K^{-1}, in the temperature range of 1134–1500 K [24], which corresponds to the temperature range from an undercooling of 202 K to a superheating of 164 K. In Wilde's experiments, the temperature dependence of the specific heat for liquid gold is so small that it only leads to a variation of 1.7% at a temperature interval of 364 K. It is not surprising that our MD simulation yields a constant value.

Like the case for density, the Neumann–Kopp rule does not apply to the specific heats of Au–Cu alloys. This may be ascribed to the nonlinear variation of the internal energy with the solute content and the large difference between the atomic sizes of copper and gold.

5. Conclusions

With the molecular dynamics simulation method and an EAM inter-atomic potential model, the density and specific heat of Au–Cu alloys are studied systematically in a wide composition range. The equilibrium melting temperatures of Au–Cu alloys are approximated from the change in the growth direction of a crystal–liquid sandwich structure under annealing. In the simulations of density and specific heat, the temperature ranges from 900 to 1900 K, corresponding to undercoolings of 421, 341, 274, 253 and 283 K for Cu, AuCu$_3$, AuCu, Au$_3$Cu and Au, respectively. Both the magnitude and the temperature dependence of the alloy density increase with increase of the Au concentration. The calculated excess volume from the simulation indicates that a linear approximation of alloy density according to the Neumann–Kopp rule will cause a negative deviation. Unlike the density, the specific heats of Au–Cu alloys are almost constant and show very weak temperature dependences over the whole temperature range from 900 to 1900 K: 530.03 ± 2.97, 351.38 ± 1.65, 262.79 ± 1.66, 209.95 ± 0.66 and 174.12 ± 1.95 J kg^{-1} K^{-1} for the five Au–Cu alloys respectively. Like for the density, the Neumann–Kopp rule is not applicable to the specific heat of the Au–Cu alloy system. The specific heat increases exponentially with increase of the copper concentration. The predictions of density and specific heat are also compared with available experimental data. Comparisons show reasonable agreements between the predictions and experimental data over a wide range of temperature and concentration. This indicates that the MD simulation is an

practicable method for quantitative prediction of thermophysical properties of liquid alloys, even in the undercooled liquid regime.

References

 [1] Egry I, Lohöfer G, Gorges E and Jacobs G 1996 *J. Phys.: Condens. Matter* **8** 9363
 [2] Han X J and Wei B 2003 *Phil. Mag.* **83** 1511
 [3] Miyazaki J, Barker J A and Pound G M 1976 *J. Chem. Phys.* **64** 3364
 [4] Rahman A and Stillinger F H 1974 *Phys. Rev.* A **10** 368
 [5] Mei J, Davenport J W and Fernando G W 1991 *Phys. Rev.* B **43** 4653
 [6] Johnson R A 1988 *Phys. Rev.* B **37** 3924
 [7] Straub G K, Schiferl S K and Wallace D C 1983 *Phys. Rev.* B **28** 312
 [8] Bhuiyan G M and Khaleque M A 1998 *J. Non-Cryst. Solids* **226** 175
 [9] Teichler H 1996 *Phys. Rev. Lett.* **76** 62
[10] Teichler H 1999 *Phys. Rev.* B **59** 8473
[11] Toxvaerd S and Praestgaard E 1977 *J. Chem. Phys.* **67** 5291
[12] Hiwatari Y, Stoll E and Schneider T 1978 *J. Chem. Phys.* **68** 3401
[13] Nagel L J, Anthony L and Futz B 1995 *Phil. Mag. Lett.* **72** 421
[14] Wei S H, Mbaye A A, Ferreira L G and Zunger A 1987 *Phys. Rev.* B **36** 4163
[15] Cai J and Ye Y Y 1996 *Phys. Rev.* B **54** 8398
[16] Polatoglou H M and Bleris G L 1994 *Solid State Commun.* **90** 425
[17] Daw M S and Baskes M L 1984 *Phys. Rev.* B **29** 6443
[18] Daw M S and Baskes M I 1983 *Phys. Rev. Lett.* **50** 1285
[19] Barrera G D, Tendler R H d and Isoardi E P 2000 *Modelling Simul. Mater. Sci. Eng.* **8** 389
[20] Allen M D and Tildesley D J 1987 *Computer Simulation of Liquids* (New York: Oxford University Press) p 47
[21] Smithells C J 1991 *Smithells Metals Reference Book* ed E A Brandes (London: Butterworths) pp 11–72
[22] Smithells C J 1991 *Smithells Metals Reference Book* ed E A Brandes (London: Butterworths) pp 14–6
[23] Bykov A and Pastukhov E 2000 *J. Therm. Anal. Calorim.* **60** 845
[24] Wilde G, Mitsch C, Görler G P and Willnecker R 1996 *J. Non-Cryst. Solids* **205–207** 425